JOURNAL OF GEOPHYSICAL RESEARCH, VOL. 99, NO. D7, PAGES 14,415–14,428, JULY 20, 1994

A simple hydrologically based model of land surface water and energy fluxes for general circulation models

Xu Liang and Dennis P. Lettenmaier

Department of Civil Engineering, University of Washington, Seattle

Eric F. Wood

Department of Civil Engineering and Operations Research, Princeton University, Princeton, New Jersey

Stephen J. Burges

Department of Civil Engineering, University of Washington, Seattle

Abstract. A generalization of the single soil layer variable infiltration capacity (VIC) land surface hydrological model previously implemented in the Geophysical Fluid Dynamics Laboratory general circulation model (GCM) is described. The new model is comprised of a two-layer characterization of the soil column, and uses an aerodynamic representation of the latent and sensible heat fluxes at the land surface. The infiltration algorithm for the upper layer is essentially the same as for the single layer VIC model, while the lower layer drainage formulation is of the form previously implemented in the Max-Planck-Institut GCM. The model partitions the area of interest (e.g., grid cell) into multiple land surface cover types; for each land cover type the fraction of roots in the upper and lower zone is specified. Evapotranspiration consists of three components: canopy evaporation, evaporation from bare soils, and transpiration, which is represented using a canopy and architectural resistance formulation. Once the latent heat flux has been computed, the surface energy balance is iterated to solve for the land surface temperature at each time step. The model was tested using long-term hydrologic and climatological data for Kings Creek, Kansas to estimate and validate the hydrological parameters, and surface flux data from three First International Satellite Land Surface Climatology Project Field Experiment intensive field campaigns in the summer-fall of 1987 to validate the surface energy fluxes.

1. Introduction

The problem of how to represent the land surface in general circulation models (GCMs) used for climate simulation and numerical weather prediction has drawn the interest of climate modelers, and increasingly, hydrologists and systems ecologists. *Manabe* [1969] used Budyko's "bucket" model to represent land surface hydrology at the global scale, and variations of the bucket model have been used in most GCMs. Recent improvements in GCM land surface representations have been primarily in the area of soil-vegetation-atmosphere transfer schemes (SVATS) which seek to represent the interactions of vegetation with the soil column and the atmosphere as they affect surface energy fluxes, especially latent heat. Among the best known SVATS are biosphere-atmosphere transfer scheme (BATS) [*Dickinson et al.*, 1986] and simple biosphere model (SiB) [*Sellers et al.*, 1986]. A distinguishing feature of SVATS, which is evident in both BATS and SiB, is that they have a high level of vertical resolution and structure, but a low level of horizontal resolution [*Wood*, 1991]. In addition, most SVATS use a "flat Earth" representation of the land surface. Topography can significantly affect large scale soil moisture dynamics, runoff production, and surface energy fluxes (J.S. Famiglietti and E.F. Wood, Application of multiscale water and energy balance model on a tall grass prairie, submitted to *Water Resources Research*, 1993, herein after referred to as Familglietti and Wood, submitted paper 1).

An alternative line of investigation is to develop simpler land surface models that still incorporate important features of the governing hydrological processes in both the vertical and horizontal. For example, *Xue et al.* [1991] simplified SiB by reducing the number of parameters from 44 to 21, apparently with negligible loss of accuracy. *Ducoudre et al.* [1993] developed a new set of parameterizations of the hydrologic exchanges (SECHIBA) at the land/atmosphere interface within a GCM which represents vegetation, as does a recent modification to the land surface scheme of the European Center for Medium Range Weather Forecasting.

In addition to the above-noted initiatives in SVATS modeling, investigations of subgrid scale variability associated

Copyright 1994 by the American Geophysical Union.

Paper number 94JD00483.
0148-0227/94/94JD-00483$05.00

with terrain, soil and vegetation heterogeneities have been motivated by studies such as that of *Avissar and Pielke* [1989] who showed that spatial heterogeneity in vegetation can have significant effects on temperature and precipitation. *Entekhabi and Eagleson* [1989] examined the effects of subgrid spatial variability of soil moisture and storm precipitation via statistically derived expressions for the hydrologic fluxes based on the assumed subgrid soil and precipitation variability. J.S. Famiglietti and E.F. Wood (Multiscale modeling of spatially variable water and energy balance processes, submitted to *Water Resources Research*, 1993) developed a model of water and energy balance based on the concept of a topographic index, which allows the local fluxes of each grid element to be aggregated by statistical integration of the local fluxes over their respective spatial probability density functions.

In this paper we describe a land surface hydrological model suitable for incorporation in GCMs that is a generalization of the variable infiltration capacity (VIC) model described by *Wood et al.* [1992] and implemented in the Geophysical Fluid Dynamics Laboratory (GFDL)-GCM by *Stamm et al.* [1994]. The soil moisture algorithm is a generalization of the Arno model [*Francini and Pacciani*, 1991] in which the infiltration, evaporation, soil moisture and runoff generation vary within an area (or within a grid cell in GCMs). Simplifications of the Arno model, using the traditional beta function representation of evapotranspiration, have previously been incorporated in GCMs [*Stamm et al.*, 1994; *Dümenil and Todini*, 1992]. However, there are major differences between the two-layer VIC model developed here and the earlier versions incorporated in the GFDL and Max-Planck-Institut (MPI) GCMs. Both of the earlier schemes have a single soil layer, and neither explicitly represents vegetation in the surface energy flux. *Stamm et al.* [1994] concluded that "... the results over North American and Eurasia [suggest] the need to represent the surface hydrology with a two layer soil system ..."

The current model is comprised of a simple two-layer characterization of the soil column and uses an aerodynamic representation of the latent and sensible heat fluxes at the land surface based on a simplified SVATS-type representation of vegetation cover. The infiltration algorithm in the VIC model can be interpreted within the context of a spatial distribution of soils of varying infiltration capacities. It allows different types of vegetation to be present simultaneously. It does not, at present, account for the spatial variability in precipitation.

2. Model Description

The model characterizes the subsurface as consisting of two soil layers. The surface is described by N+1 land cover types, where n = 1, 2, . . . , N represents N different types of vegetation, and n = N+1 represents bare soil. There is no restriction on the number of vegetation types, but in the interest of model parsimony, N will almost always be less than 10. The vertical and horizontal characterizations are shown schematically in Figure 1. The land cover types are specified by their leaf area index (LAI), canopy resistance, and relative fraction of roots in each of the two soil layers. The evapotranspiration from each vegetation type is characterized by potential evapotranspiration, together with canopy resistance, aerodynamic resistance to the transfer of water, and architectural resistance. Associated with each land cover class is a single canopy layer, soil layer 1 (upper zone) and soil layer 2 (lower zone). The upper layer (soil layer 1) is designed to represent the dynamic behavior of the soil column that responds to rainfall events, and the lower layer (soil layer 2) is used to characterize the slowly varying between-storm soil moisture behavior. The lower layer only responds to rainfall when the upper layer is wetted and thus can separate the subsurface flow from storm quick response. Roots can extend to layer 1 or layers 1 and 2, depending on the vegetation and soil type. For the bare soil class, there is no canopy layer. In the present form of the model, the soil characteristics (that is, the distribution of water holding capacities, as described below) are the same for all land cover classes. However, each cover class may have different soil moisture distributions at each time step. Infiltration, drainage of moisture from layer 1 to layer 2, surface runoff and subsurface runoff are computed for each cover type. The total latent heat flux transferred to the atmosphere, total sensible heat and ground heat fluxes, the effective surface temperature, and the total surface runoff and subsurface runoff are then obtained by summing over all of the surface cover classes.

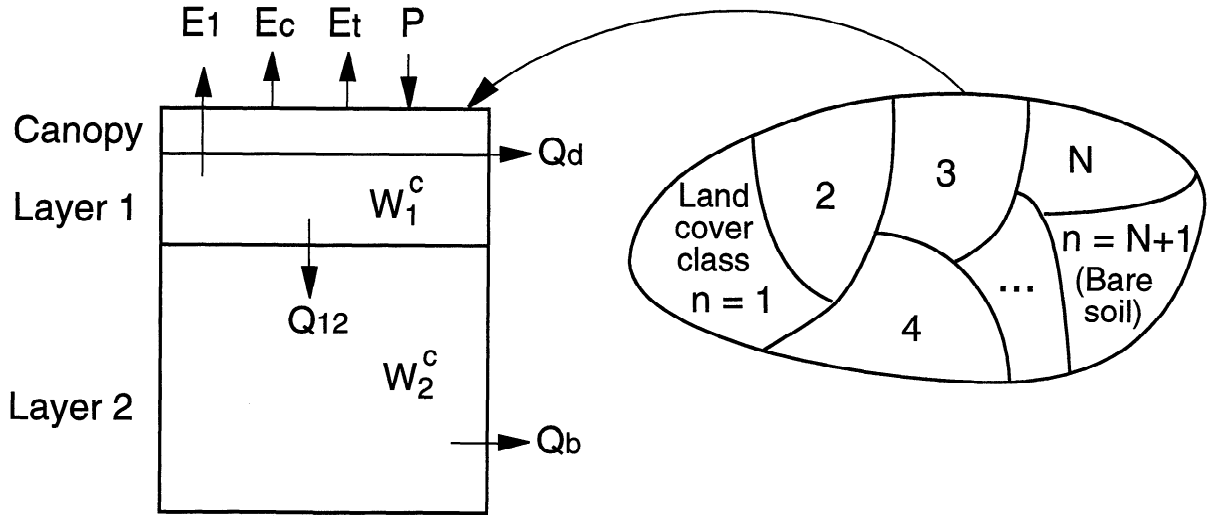

Figure 1. Schematic representation of the two-layer VIC model.

2.1. Evapotranspiration

Three types of evaporation are considered in the model. They are evaporation from the canopy layer of each vegetation class, transpiration from each of the vegetation classes, and evaporation from bare soil. Total evapotranspiration over the grid cell is computed as the sum of the canopy, vegetation, and bare soil components, weighted by the respective surface cover area fractions (equation (23)).

The maximum canopy evaporation for the nth surface cover class, $E_c^*[n]$, is specified as

$$E_c^*[n] = \left(\frac{W_i[n]}{W_{im}[n]}\right)^{2/3} E_p[n] \frac{r_w[n]}{r_w[n] + r_0[n]} \tag{1}$$

In equation (1), the argument n refers to the vegetation surface cover class index. Throughout the remainder of the paper the dependence of many of the surface and subsurface characteristics on surface cover class is implied by this argument even if not noted specifically. $W_i[n]$ is the amount of intercepted water in storage in the canopy layer, $W_{im}[n]$ is the maximum amount of water that the canopy layer can intercept; the power of 2/3 is used according to *Deardorff* [1978]. $E_p[n]$ is the potential evaporation from a surface based on the Penman-Monteith equation with the canopy resistance set to zero [*Shuttleworth*, 1993]. The architectural resistance that is due to the variation of the gradient of specific humidity between the leaves and the overlying air in the canopy layer is $r_0[n]$ [*Saugier and Katerji*, 1991], and $r_w[n]$ is the aerodynamic resistance to the transfer of water. The form of equation (1) is sometimes referred to as a "beta" representation.

The maximum amount of water intercepted by the canopy can be calculated using [*Dickinson*, 1984]

$$W_{im}[n] = K_L \times \mathrm{LAI}[n,m] \tag{2}$$

where LAI$[n,m]$ is leaf area index for the nth surface cover class in month m, and K_L is a constant, taken to be 0.2 mm following *Dickinson* [1984].

The aerodynamic resistance to the transfer of water is calculated as [*Monteith and Unsworth*, 1990]

$$r_w[n] = \frac{1}{C_w[n] u_n(z_2)} \tag{3}$$

where $u_n(z_2)$ is the wind speed over the nth surface cover class at level $z_2[n]$, and $C_w[n]$ is the transfer coefficient for water which is estimated taking into account the atmospheric stability [*Louis*, 1979] as follows:

$$C_w[n] = 1.351 \times a^2[n] \times F_w[n] \tag{4a}$$

where

$$a^2[n] = \frac{K^2}{\left[\ln\left(\frac{z_2[n] - d_0[n]}{z_0[n]}\right)\right]^2} \tag{4b}$$

is the drag coefficient for the case of near-neutral stability, K is von Karman's constant, which we take as 0.4; $d_0[n]$ is the zero plane displacement height, and $z_0[n]$ is the roughness length.

Following *Louis* [1979], $F_w[n]$ is defined as

$$F_w[n] = 1 - \frac{9.4 Ri_B[n]}{1 + c \cdot \left|Ri_B[n]\right|^{1/2}}, \quad Ri_B[n] < 0 \tag{4c}$$

$$F_w[n] = \frac{1}{\left(1 + 4.7 Ri_B[n]\right)^2}, \quad 0 \le Ri_B[n] \le 0.2 \tag{4d}$$

where $Ri_B[n]$ is the bulk Richardson number, and c is expressed as

$$c = 49.82 \times a^2[n] \times \left(\frac{z_2[n] - d_0[n]}{z_0[n]}\right)^{1/2} \tag{4e}$$

In Louis' representation, the drag coefficients for water and heat are taken to be equal, but they can be different from the drag coefficient for momentum.

Based on the formulation of *Blondin* [1991] and *Ducoudre et al.* [1993], transpiration is estimated as

$$E_t[n] = \left[1 - \left(\frac{W_i[n]}{W_{im}[n]}\right)^{2/3}\right] E_p[n] \frac{r_w[n]}{r_w[n] + r_0[n] + r_c[n]} \tag{5}$$

where $r_c[n]$ is the canopy resistance given by

$$r_c[n] = \frac{r_{0c}[n] g_{sm}[n]}{\mathrm{LAI}[n,m]} \tag{6}$$

In equation (6), $r_{0c}[n]$ is the minimum canopy resistance, $g_{sm}[n]$ is a soil moisture stress factor depending on the water availability in the root zone for the nth surface cover class. It is expressed as

$$g_{sm}^{-1}[n] = 1, \qquad W_j[n] \ge W_j^{cr} \tag{7a}$$

$$g_{sm}^{-1}[n] = \frac{W_j[n] - W_j^w}{W_j^{cr} - W_j^w}, \qquad W_j^w \le W_j[n] < W_j^{cr} \tag{7b}$$

$$g_{sm}^{-1}[n] = 0, \qquad W_j[n] < W_j^w \tag{7c}$$

where $W_j[n]$ is the soil moisture content in layer j, j=1, 2. W_j^{cr} is the critical value above which transpiration is not affected by the moisture stress in the soil, and W_j^w is the soil moisture content at permanent wilting point. Water can be extracted from layers 1 and/or 2 depending on the fractions of roots $f_1[n]$ and $f_2[n]$ in each layer.

There is no soil moisture stress, i.e., $g_{sm}[n]$=1 in equation (6), if either (i) $W_2[n]$ is greater or equal to W_2^{cr}, and $f_2[n] \ge 0.5$ or (ii) $W_1[n]$ is greater or equal to W_1^{cr}, and $f_1[n] \ge 0.5$. In case (i), the transpiration is supplied by layer 2 with no soil moisture stress, i.e., $E_t[n] = E_2^t[n]$ (regardless of water availability in layer 1); in case (ii), the transpiration takes water from layer 1, i.e., $E_t[n] = E_1^t[n]$, also without any soil moisture stress. Otherwise, transpiration is

$$E_t[n] = f_1[n] \cdot E_1^t[n] + f_2[n] \cdot E_2^t[n] \tag{8}$$

where $E_1^t[n]$, $E_2^t[n]$ are the transpiration from layer 1 and layer

2, respectively, computed using equation (5). If the roots only extend to layer 1, then $E_t[n]=E_1^t[n]$ with $f_2[n] = 0$.

For the case of a continuous rainfall with a rate lower than the canopy evaporation, it is important to consider evaporation from the vegetation when there is insufficient intercepted water to supply the atmospheric demand within one time step. In this case, the evaporation from the canopy layer, $E_c[n]$, is

$$E_c[n] = f[n]\cdot E_c^*[n] \tag{9}$$

where $f[n]$ is the fraction of the time step required for canopy evaporation to exhaust the canopy interception storage. It is given by

$$f[n] = \min\left(1, \frac{W_i[n]+P\cdot\Delta t}{E_c^*[n]\cdot\Delta t}\right) \tag{10}$$

where P is the precipitation rate, and Δt is the time step which is taken as 1 hour in the model calculation. The transpiration during the time step is then

$$E_t[n] = (1.0-f[n])E_p[n]\frac{r_w[n]}{r_w[n]+r_0[n]+r_c[n]} + f[n]\cdot\left[1-\left(\frac{W_i[n]}{W_{im}[n]}\right)^{2/3}\right]E_p[n]\frac{r_w[n]}{r_w[n]+r_0[n]+r_c[n]} \tag{11}$$

where the first term represents the fraction of the time step for which no evaporation occurs from the canopy interception storage, and the second term represents the fraction of the time step for which both evaporation from the canopy and transpiration occur.

Evaporation from bare soil is extracted only from layer 1; bare soil evaporation from layer 2 (E_2) is assumed to be zero. When layer 1 is saturated, it evaporates at the potential rate $E_p[N+1]$,

$$E_1 = E_p[N+1] \tag{12}$$

when it is unsaturated, it evaporates at rate E_1 which varies within the bare soil area due to the inhomogeneities in infiltration, topography and soil characteristics. E_1 is computed using the evaporation formulation of *Francini and Pacciani* [1991]. This formulation uses the structure of the Xinanjiang model [*Zhao et al.*, 1980] (see also *Wood et al.* [1992]) and assumes that the infiltration capacity varies within an area and can be expressed as

$$i = i_m\left[1-(1-A)^{1/b_i}\right] \tag{13}$$

where i and i_m are the infiltration capacity and maximum infiltration capacity, respectively, A is the fraction of an area for which the infiltration capacity is less than i, and b_i is the infiltration shape parameter. Let A_s represent the fraction of the bare soil that is saturated, and i_0 represent the corresponding point infiltration capacity. Then, as suggested by Figure 2, E_1 can be expressed as

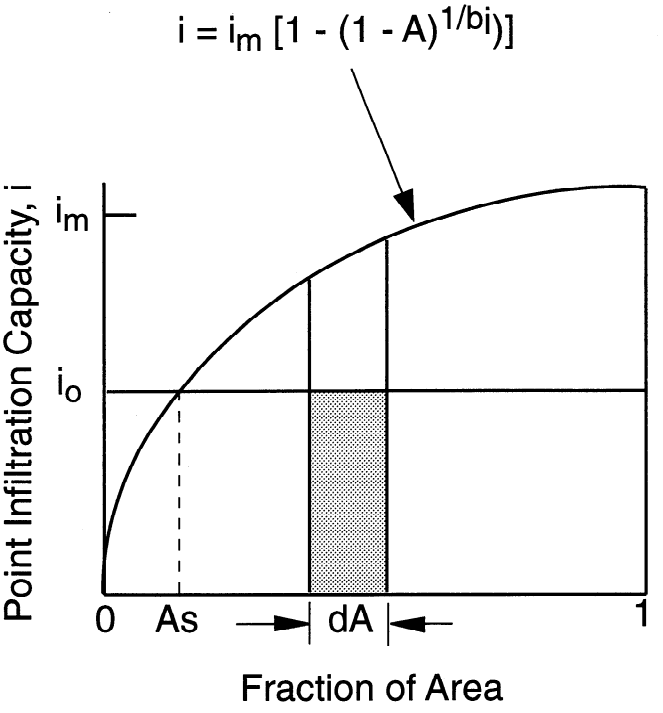

Figure 2. Schematic representation of the computation of evaporation from bare soil.

$$E_1 = E_p[N+1]\left\{\int_0^{A_s} dA + \int_{A_s}^{1}\frac{i_0}{i_m\left[1-(1-A)^{1/b_i}\right]}dA\right\} \tag{14}$$

In equation (14), the first integral represents the contribution of the saturated area, which evaporates at the potential rate. Since there is no analytical expression for the second integral in equation (14), E_1 is obtained through a power series expansion:

$$E_1 = E_p[N+1]\left\{A_s + \frac{i_0}{i_m}(1-A_s)\left[1+\frac{b_i}{1+b_i}(1-A_s)^{1/b_i} + \frac{b_i}{2+b_i}(1-A_s)^{2/b_i} + \frac{b_i}{3+b_i}(1-A_s)^{3/b_i} + \cdots\right]\right\} \tag{15}$$

This approach accounts for the subgrid variability in soil moisture within the area covered by bare soil.

2.2. Canopy Layer Water Balance

The water balance in the canopy layer (interception) can be described by

$$\frac{dW_i[n]}{dt} = P - E_c[n] - P_t[n],\quad 0 \le W_i[n] \le W_{im}[n] \tag{16}$$

where $P_t[n]$ is the throughfall of precipitation which occurs when $W_{im}[n]$ is exceeded for the nth surface cover class.

2.3. Surface Runoff From Bare Soil

Surface runoff is computed using the formulation for infiltration given by equation (13). The Xinanjiang formulation, which is described in detail by *Wood et al.* [1992],

is assumed to hold for the upper soil layer only. The maximum soil moisture content of layer 1, W_1^c, is related to i_m and b_i as follows:

$$W_1^c = \frac{i_m}{1+b_i} \tag{17}$$

The Xinanjiang model effectively assumes that runoff is generated by those areas for which precipitation, when added to soil moisture storage at the end of the previous time step, exceeds the storage capacity of the soil. The direct runoff from these areas is $Q_d[N+1]$, where $N+1$ indicates the bare soil class. In integrated form, the result is

$$Q_d[N+1]\cdot\Delta t = P\cdot\Delta t - W_1^c + W_1^-[N+1], \quad i_0 + P\cdot\Delta t \geq i_m \tag{18a}$$

$$Q_d[N+1]\cdot\Delta t = P\cdot\Delta t - W_1^c + W_1^-[N+1] + W_1^c\left[1-\frac{i_0+P\cdot\Delta t}{i_m}\right]^{1+b_i}, \quad i_0 + P\cdot\Delta t \leq i_m \tag{18b}$$

where $W_1^-[N+1]$ is the soil moisture content in layer 1 at the beginning of the time step. Note that, for the bare soil class, there is no canopy storage, hence "throughfall" is equal to precipitation P. For bare soil, the water balance in layer 1 is

$$W_1^+[N+1] = W_1^-[N+1] + \left(P - Q_d[N+1] - Q_{12}[N+1] - E_1\right)\cdot\Delta t \tag{19}$$

where $W_1^+[N+1]$ is the soil moisture content in layer 1 at the end of each time step, and $Q_{12}[N+1]$ is the drainage from layer 1 to layer 2. Assuming that the drainage is driven by gravity, we use the *Brooks and Corey* [1964] relation to estimate the hydraulic conductivity, and thus we can express the drainage from layer 1 to layer 2 as

$$Q_{12}[N+1] = K_s\left(\frac{W_1[N+1]-\theta_r}{W_1^c-\theta_r}\right)^{\frac{2}{B_p}+3} \tag{20}$$

where K_s is the saturated hydraulic conductivity, θ_r is the residual moisture content, and B_p is the pore size distribution index.

2.4. Subsurface Runoff From Bare Soil

The formulation of subsurface runoff (base flow) follows the Arno model conceptualization [*Francini and Pacciani*, 1991], which is applied only to the lower soil layer (drainage from layer 1 goes only to layer 2, and does not contribute to runoff). Base flow is given by

$$Q_b[N+1] = \frac{D_s D_m}{W_s W_2^c} W_2^-[N+1], \quad 0 \leq W_2^-[N+1] \leq W_s W_2^c \tag{21a}$$

$$Q_b[N+1] = \frac{D_s D_m}{W_s W_2^c} W_2^-[N+1] + \left(D_m - \frac{D_s D_m}{W_s}\right)\left(\frac{W_2^-[N+1]-W_s W_2^c}{W_2^c - W_s W_2^c}\right)^2, \quad W_2^-[N+1] \geq W_s W_2^c \tag{21b}$$

where $Q_b[N+1]$ is the subsurface runoff, D_m is the maximum subsurface flow, D_s is a fraction of D_m, W_2^c is the maximum soil moisture content of layer 2, W_s is a fraction of W_2^c, with $D_s \leq W_s$, and $W_2^-[N+1]$ is the soil moisture content at the beginning of the time step in layer 2. Equations (21a) and (21b) describe a recession that is linear below a threshold (equation (21a)), and nonlinear at higher soil moisture values (equation (21b)) as shown in Figure 3. The nonlinear drainage is required to represent situations where substantial subsurface storm flow occurs. Equations (21a) and (21b) have a continuous first derivative at the transition from the linear to nonlinear drainage as shown in Figure 3.

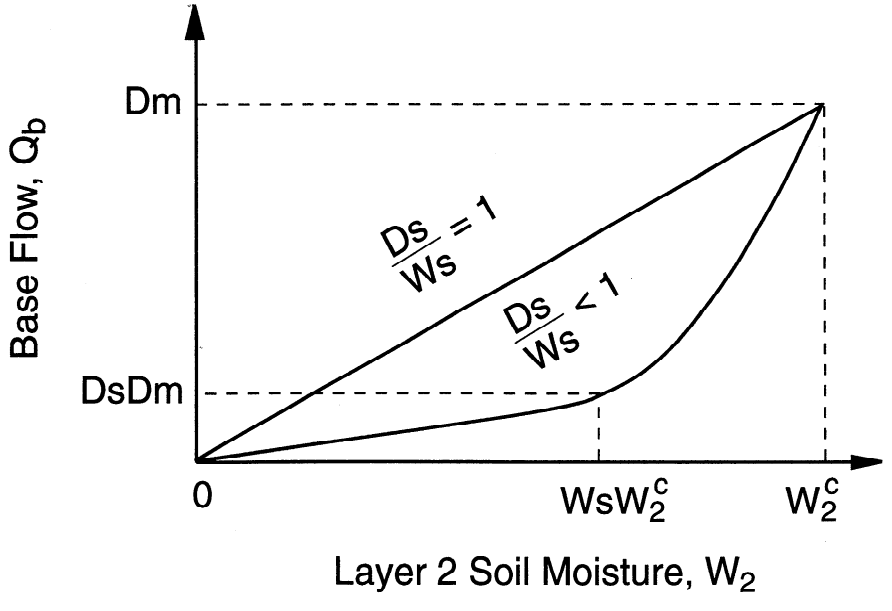

Figure 3. Schematic representation of Arno nonlinear base flow.

Using equations (21a) and (21b), and the notation that $W_2^+[N+1]$ is the layer 2 soil moisture content at the end of the current time, the water balance is

$$W_2^+[N+1] = W_2^-[N+1] + \left(Q_{12}[N+1] - Q_b[N+1] - E_2\right)\cdot\Delta t \tag{22a}$$

when $W_2^-[N+1] + (Q_{12}[N+1] - Q_b[N+1] - E_2)\cdot\Delta t < W_2^c$, in which case Q_b is given by equation (21a) or (21b).

In the case $W_2^-[N+1] + (Q_{12}[N+1] - Q_b'[N+1] - E_2)\cdot\Delta t > W_2^c$, (where $Q_b'[N+1]$ is given by equation (21a) or (21b)),

$$W_2^+[N+1] = W_2^c \tag{22b}$$

and

$$Q_b''[N+1] = W_2^-[N+1] + \left(Q_{12}[N+1] - Q_b'[N+1] - E_2\right)\cdot\Delta t - W_2^c$$

When equation (22b) applies, the total subsurface runoff from layer 2 is given by $Q_b[N+1] = Q_b'[N+1] + Q_b''[N+1]$. In practice, this condition occurs rarely.

2.5. Surface and Subsurface Runoff From Soil With Vegetation Cover

The equations for surface and subsurface flow and the water balance in each layer are the same for cover classes with vegetation as for the bare soil case, except that P, E_1, and E_2 are changed to $P_t[n]$, $E_1^t[n]$, and $E_2^t[n]$, respectively, in equations (18), (19), and (22), to reflect the vegetation class. The total evapotranspiration E, and the total runoff Q can be then expressed as

$$E = \sum_{n=1}^{N} C_v[n]\cdot\left(E_c[n] + E_t[n]\right) + C_v[N+1]\cdot E_1 \tag{23}$$

$$Q = \sum_{n=1}^{N+1} C_v[n]\cdot\left(Q_d[n] + Q_b[n]\right) \tag{24}$$

where $C_v[n]$ is the fraction of vegetation cover for the nth (n=1, 2, . . . , N) surface cover class of interest, $C_v[N+1]$ is the fraction of the bare soil covered area, and $\sum_{n=1}^{N+1} C_v[n] = 1$.

2.6. Aerodynamic Flux Representation

The two-layer hydrological model described above is used in conjunction with the energy balance at the land surface and the thermal properties of soils to calculate the surface temperature, and simultaneously, the fluxes of sensible heat and ground heat which depend on surface temperature. The energy balance equation for an ideal surface of the nth surface cover class can be expressed as

$$R_n[n] = H[n] + \rho_w L_e E[n] + G[n] \tag{25}$$

with

$$E[n] = E_c[n] + E_t[n], \quad n = 1, 2, \ldots, N \tag{26a}$$

$$E[N+1] = E_1 \tag{26b}$$

where $R_n[n]$ is the net radiation, $H[n]$ is the sensible heat flux, ρ_w is the density of liquid water, L_e is the latent heat of vaporization, $\rho_w L_e E[n]$ is the latent heat flux (e.g., with units of Wm^{-2}), and $G[n]$ is the ground heat flux. For a surface that is relatively flat and homogeneous, the energy balance equation for a layer of the air column bounded by the ground surface at the bottom and a surface of given height in the atmosphere above, can be expressed as

$$R_n[n] = H[n] + \rho_w L_e E[n] + G[n] + \Delta H_s[n] \tag{27}$$

where $\Delta H_s[n]$ is the change in the energy storage in the layer per unit time, per unit area. The sensible and latent heat fluxes, as well as the net radiation, are associated with the top surface of the air layer, and the ground heat flux with the bottom of the layer. The rate of heat energy storage in the layer is

$$\Delta H_s[n] = \frac{\rho_a c_p\left(T_s^+[n] - T_s^-[n]\right) z_a[n]}{2\Delta t} \tag{28}$$

where ρ_a and c_p are the mass density and specific heat of air at constant pressure, $T_s^+[n]$ and $T_s^-[n]$ are the surface temperature of the bottom surface of the layer at the end and at the beginning of a time step, respectively, and $z_a[n]$ is the height of the top surface of the layer which is used only when $\Delta H_s[n]$ is considered to be significant.

The net radiation is given by

$$R_n[n] = \left(1 - \alpha[n]\right)R_s + \varepsilon[n]\cdot\left(R_L - \sigma T_s^4[n]\right) \tag{29}$$

where $\alpha[n]$ is the albedo of the nth surface cover class, R_s is the downward shortwave radiation, $\varepsilon[n]$ is the emissivity of the nth surface cover class, R_L is the downward long-wave radiation, and σ is the Stefan-Boltzmann constant. The latent heat flux, which is the link between the water and energy balances, is obtained from equation (26). The sensible heat flux is given by

$$H[n] = \frac{\rho_a c_p}{r_h[n]}\left(T_s[n] - T_a[n]\right) \tag{30}$$

where $T_s[n]$ is the surface temperature, $T_a[n]$ is the air temperature, and $r_h[n]$ is the aerodynamic resistance to heat flow. We take $r_h[n]$ to be equal to $r_w[n]$ in equation (3). The ground heat flux $G[n]$ is estimated using two thermal soil layers. For the first soil layer, with depth D_1 (subsequently assumed to be 50 mm), we have

$$G[n] = \frac{\kappa[n]}{D_1}\left(T_s[n] - T_1[n]\right) \tag{31}$$

where $\kappa[n]$ is the soil thermal conductivity, and $T_1[n]$ is the soil temperature at depth D_1. For the second soil layer with depth D_2, at which the bottom boundary condition is constant soil temperature, the law of energy conservation (assuming that the heat storage in the first soil thermal layer is negligible) gives

$$\frac{C_s[n]\cdot\left(T_1^+[n] - T_1^-[n]\right)}{2\cdot\Delta t} = \frac{G[n]}{D_2} - \frac{\kappa[n]\cdot\left(T_1[n] - T_2\right)}{D_2^2} \tag{32}$$

where $C_s[n]$ is the soil heat capacity, $T_1^+[n]$ and $T_1^-[n]$ are the

soil temperature at depth D_1 at the end and the beginning of a time step, respectively, and T_2 is the constant temperature at depth D_2. At present, $C_s[n]$ and $\kappa[n]$ are not considered to be functions of the soil water content (although such an adjustment would be straightforward), and are taken to be the same for both soil thermal layers. From equations (31) and (32), the ground heat flux $G[n]$ can be expressed as

$$G[n] = \frac{\frac{\kappa[n]}{D_2}\left(T_s[n] - T_2\right) + \frac{C_s[n]\cdot D_2}{2\cdot\Delta t}\left(T_s[n] - T_1^-[n]\right)}{1 + \frac{D_1}{D_2} + \frac{C_s[n]\cdot D_1\cdot D_2}{2\cdot\Delta t\cdot\kappa[n]}} \tag{33}$$

For the case where $\Delta H_s[n]$ can be ignored, the energy balance equation for an ideal surface (equation (25)) can be used instead of equation (27). From equations (29), (30), (33), and equation (26) (scaled by the latent heat of vaporization and the density of liquid water), the sensible heat and ground heat fluxes and the surface temperature for the nth cover class can be obtained. In the case where $\Delta H_s[n]$ is negligible, the surface temperature $T_s[n]$ is iteratively solved using equation (34):

$$\varepsilon[n]\sigma T_s^4[n] + \left(\frac{\rho_a c_p}{r_h[n]} + \frac{\frac{\kappa[n]}{D_2} + \frac{C_s[n]\cdot D_2}{2\cdot\Delta t}}{1 + \frac{D_1}{D_2} + \frac{C_s[n]\cdot D_1\cdot D_2}{2\cdot\Delta t\cdot\kappa[n]}}\right)\cdot T_s[n]$$
$$= \left(1-\alpha[n]\right)R_s + \varepsilon[n]\cdot R_L + \frac{\rho_a c_p}{r_h[n]}T_a[n] - \rho_w L_e E[n]$$
$$+ \frac{\frac{\kappa[n]\cdot T_2}{D_2} + \frac{C_s[n]\cdot D_2\cdot T_1^-[n]}{2\cdot\Delta t}}{1 + \frac{D_1}{D_2} + \frac{C_s[n]\cdot D_1\cdot D_2}{2\cdot\Delta t\cdot\kappa[n]}} \tag{34}$$

For the case where $\Delta H_s[n]$ cannot be ignored, equations (27) to (30), and (33) are combined to give

$$\varepsilon[n]\sigma\left(T_s^+[n]\right)^4 + \left(\frac{\rho_a c_p}{r_h[n]} + \frac{\rho_a c_p z_a[n]}{2\cdot\Delta t}\right.$$
$$\left. + \frac{\frac{\kappa[n]}{D_2} + \frac{C_s[n]\cdot D_2}{2\cdot\Delta t}}{1 + \frac{D_1}{D_2} + \frac{C_s[n]\cdot D_1\cdot D_2}{2\cdot\Delta t\cdot\kappa[n]}}\right)\cdot T_s^+[n] =$$
$$\left(1-\alpha[n]\right)\cdot R_s + \varepsilon[n]\cdot R_L + \frac{\rho_a c_p}{r_h[n]}T_a[n] - \rho_w L_e E[n]$$
$$+ \frac{\rho_a c_p z_a[n]\cdot T_s^-[n]}{2\cdot\Delta t} + \frac{\frac{\kappa[n]\cdot T_2}{D_2} + \frac{C_s[n]\cdot D_2\cdot T_1^-[n]}{2\cdot\Delta t}}{1 + \frac{D_1}{D_2} + \frac{C_s[n]\cdot D_1\cdot D_2}{2\cdot\Delta t\cdot\kappa[n]}} \tag{35}$$

Table 1. Average Monthly NDVIs at FIFE

Month	NDVI
Jan.	53
Feb.	58
March	66
April	89
May	132
June	147
July	145
Aug.	136
Sept.	122
Oct.	84
Nov.	66
Dec.	62

$T_s[n]$ is determined in the same manner as for equation (34). The effective surface temperature T_s, sensible heat flux H, and ground heat flux G can then be obtained as

$$T_s = \sum_{n=1}^{N+1} C_v[n]\cdot T_s[n] \tag{36}$$

$$H = \sum_{n=1}^{N+1} C_v[n]\cdot H[n] \tag{37}$$

$$G = \sum_{n=1}^{N+1} C_v[n]\cdot G[n] \tag{38}$$

The iterative procedures for computing the surface temperature $T_s[n]$ is as follows:

1. Set the surface temperature to the air temperature at the first time step. This allows computation of the initial values of the bulk Richardson number, the vapor pressure deficit and net radiation that are needed in estimating $E_p[n]$ through the Penman-Monteith formulation.
2. Iterate equation (34) or (35) to solve for the surface temperature.
3. Use the surface temperature obtained from step (2) to calculate the bulk Richardson number, vapor pressure deficit, and net radiation again.
4. Recalculate the surface temperature iteratively using equation (34) or (35). The surface temperature obtained from this step is then considered to be the surface temperature at the first time step of the model simulation.
5. For subsequent time steps, use the surface temperature from the previous time step to calculate the bulk Richardson number, vapor pressure deficit, and net radiation, then repeat steps 2-4.

It should be mentioned that the procedure described above is not iterative in the same sense as the procedure used to solve for the surface temperature from equation (34) or (35), since the steps are only repeated once. The use of a single iteration is justified by the relatively smooth variation usually observed in

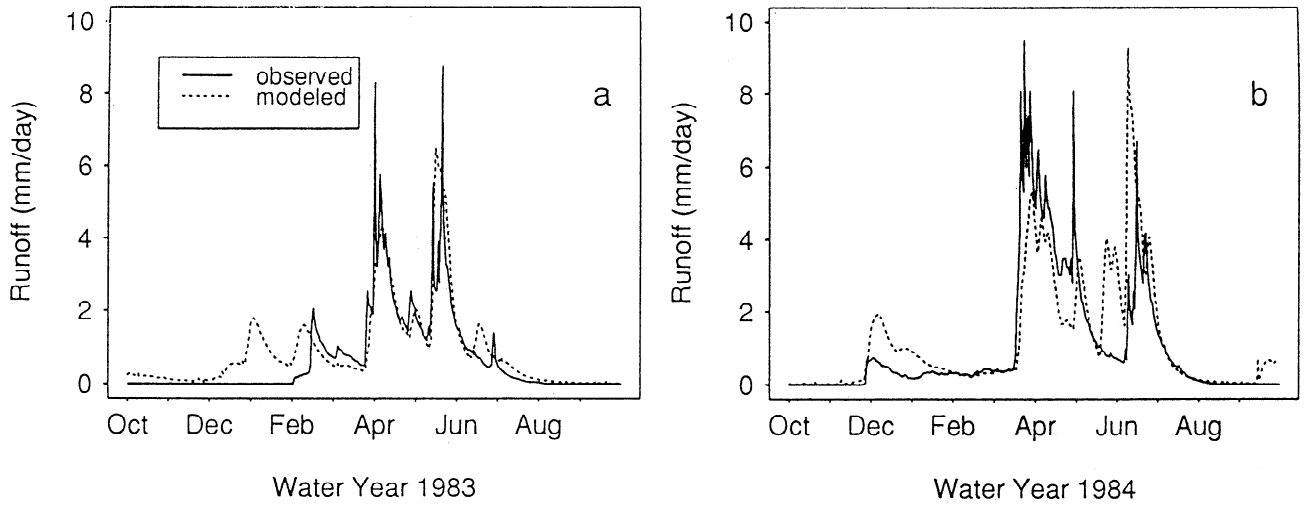

Figure 4. Predicted (dotted line) and observed (solid line) streamflow for Kings Creek for calibration years 1983-1984.

surface temperatures due to the thermal inertia of the soil column. Of course, multiple iterations could be performed if required. Such an approach in fact implies two nested iterations; one to solve equation (34) or (35), and the other to determine the bulk Richardson number and related quantities needed to compute the surface energy fluxes.

2.7. Snow

When snow is present, the model is coupled with a single-layer, energy- and mass-balance snow accumulation and ablation model [*Wigmosta et al.*, 1994]. At the snow-air interface, the energy exchange is described by the net radiation, sensible heat, evaporation from the water in the snowpack and sublimation or condensation, and the heat advected to the snowpack by rainfall. The snow-ground interface is assumed to be a zero energy flux boundary. Snow albedo is determined based on snow age. The present version of the snowmelt model does not consider fractional snow coverage; it is assumed that the entire area is covered by a uniform depth of snow if a snowpack is present.

3. Parameter Estimation

The test location for the model was the FIFE (First International Satellite and Land Surface Climatology Project Field Experiment) site in central Kansas. The FIFE experiment is described in detail by *Sellers et al.* [1992]. The site is a 15× 15 km^2 region on the Konza Prairie, a native grassland preserve near Manhattan, Kansas. It has a fairly homogeneous tall grass cover, and thus the number of vegetation types N was taken to be 1, with $C_v[N+1]=0.0$. The Kings Creek catchment, of area 11.7 km^2, lies within the FIFE site. The FIFE site is of interest because of the detailed measurements of surface fluxes that were collected in the summer of 1987. During the period May-October 1987, four intensive field campaigns (IFCs) were conducted at the site, during which tower-based measurements of latent, sensible, and ground heat fluxes were made. In addition, throughout the summer of 1987, a network of portable automated mesonet (PAM) stations was operated, from which measured values of incoming solar and long-wave radiation, and other meteorological data are available. Furthermore, long-term streamflow data exist for Kings Creek, along with long-term climatalogical data at nearby Manhattan, Kansas, which allows for validation of the hydrological portion of the VIC model. The overall strategy for validation of the model was to

Table 2. Model Parameters

Parameter	Value
b_i	0.008
D_m, mm/h	0.34
D_s	7.7×10^{-5}
W_s	0.96
B_p	0.16
K_s, mm/h	6.44
W_1^c, m	0.25
W_2^c, m	1.25
W_j^w, m	0.18 W_j^c
W_j^{cr}, m	0.46 W_j^c
θ	0.5
$r_0[1]$, s/m	2.0
$r_{0c}[1]$, s/m	100.0
$d_0[1]$, m	0.25
$z_0[1]$, m	0.07
$C_v[1]$	1.0
$f_1[1]$	1.0
$f_2[1]$	0.0
T_2, °K	293.6
$\alpha[1]$	0.2
$\kappa[1]$, W m^{-1} K^{-1}	0.514
$C_s[1]$, J m^{-3} K^{-1}	2.13×10^6

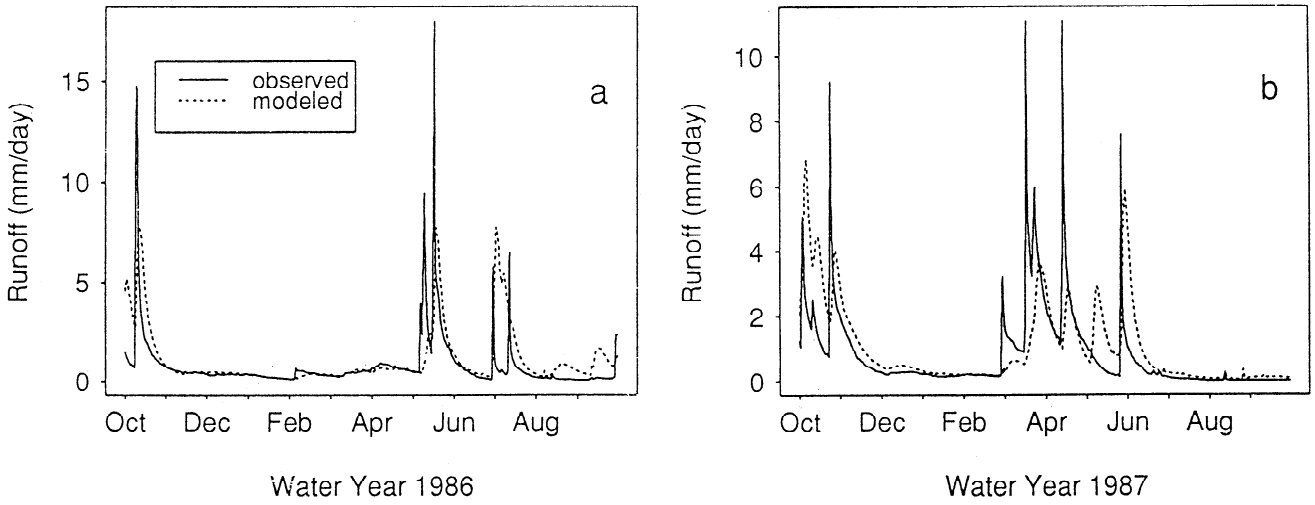

Figure 5. Predicted (dotted) and observed (solid) streamflow for Kings Creek for verification years 1986-1987.

estimate the hydrological parameters using precipitation and streamflow data for part of the long-term Kings Creek record, and to evaluate its hydrological performance using the remaining part of the record. The model's surface flux algorithms were then parameterized and validated using measured fluxes observed during the summer 1987 IFCs.

Daily precipitation and temperature maximum/ minimum data have been collected at Manhattan, Kansas, which is about 11 km from the centroid of the Kings Creek catchment, which has been gauged since the late 1800s. Daily average stream discharge data for Kings Creek (U.S. Geological Survey No. 06879650, 11.7 km^2) have been collected since about 1980. Surface meteorological and surface flux data at the FIFE site are limited to selected periods during the summer of 1987. Data from the PAM stations include surface pressure (p), mixing ratio (ω) and air temperature (T_a) at the 2-m level and wind speed (u) measured at 5.4 m above ground level, surface temperature (T_s), ground soil temperatures, T_{10} and T_{50}, at 10 cm and 50 cm below the surface, respectively, and downward short- and long-wave radiation. Radiation data were also collected from flux stations (eddy correlation and Bowen ratio). Data from both PAM stations and flux stations were averaged for each date and time among all the stations by *Betts et al.* [1993]. They found from consistency analysis of the radiation

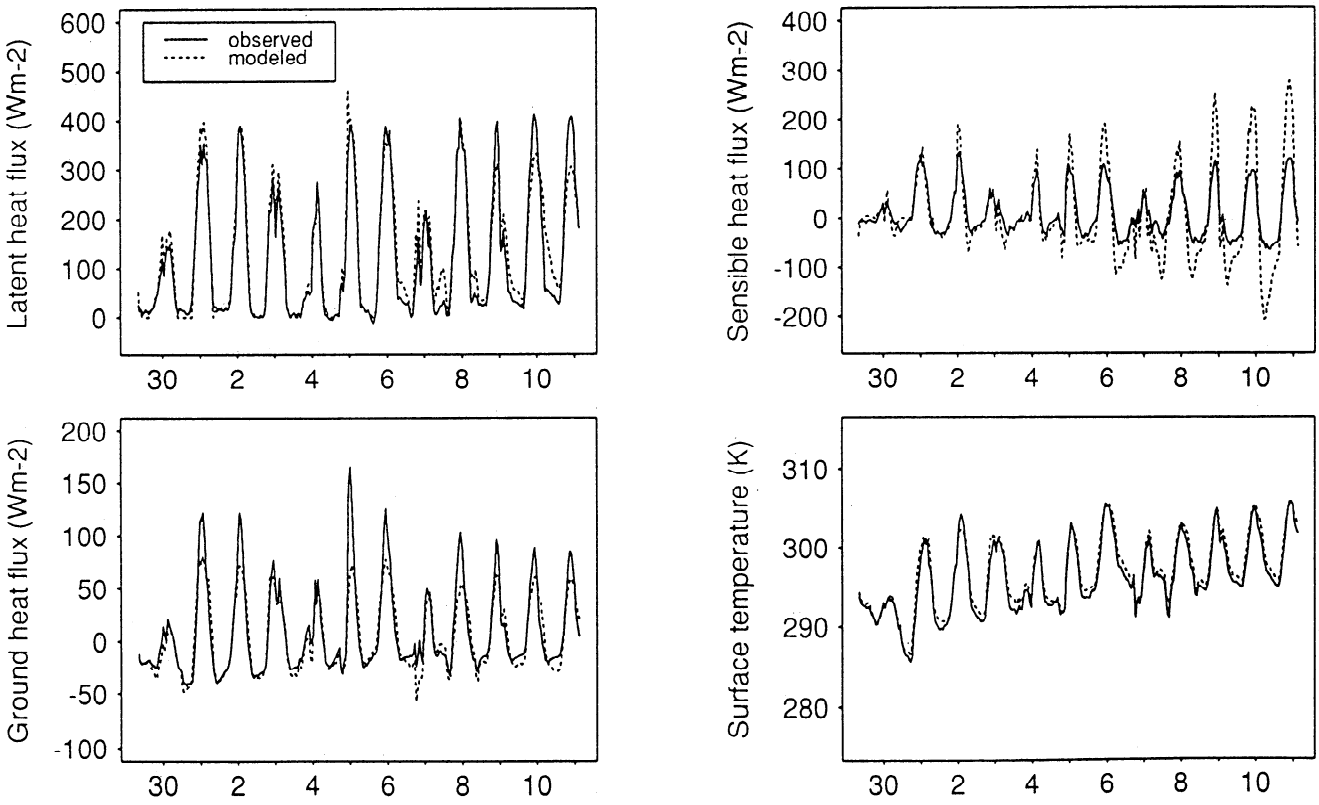

Figure 6. Comparison of predicted (dotted) and observed (solid) surface fluxes and surface temperature at the FIFE site for June 30-July 11, 1987 (IFC 2).

data that the flux data were more self-consistent internally than the PAM data based on the comparison of the calculated and measured net radiation. Therefore we used the radiation data from the flux stations and the atmospheric data from PAM stations to test our model surface flux and surface temperature predictions. Data for 35 days common to the two data sets in the summer of 1987 were used. They are June 30-July 11, August 9-20, and October 6-16.

The model parameters can be classified into hydrological parameters and atmospherically related parameters. The hydrological parameters include the infiltration shape parameter b_i (equation (13)), the soil pore size distribution index B_p, the residual moisture content θ_r, the saturated hydraulic conductivity K_s (equation (20)), the three base flow related parameters D_s, D_m, and W_s (equation (21)), the maximum soil moisture contents W_1^c and W_2^c in layers 1 and 2, respectively (equations (17) and (21)), the soil moisture content at the wilting point W_j^w and at the critical point W_j^{cr} (j=1,2) in equation (7). Atmospherically related parameters include architectural resistance $r_0[n]$ (equation (1)), minimum canopy resistance $r_{0c}[n]$ (equation (6)), leaf area index LAI[n,m] (n=1, 2, . . . , N; m=1, 2, . . . , 12) for each surface cover class (equation (6)), the zero plane displacement height $d_0[n]$, roughness length $z_0[n]$ (equation (4a)), and the relative fraction of roots in each of the two soil zones $f_1[n]$ and $f_2[n]$ (equation (8)). We classify $f_1[n]$ and $f_2[n]$ as atmospherically related parameters because they determine the canopy resistance (equations (6)-(8)).

Among the hydrological parameters, only three (b_i, D_s, and W_s) would best be estimated using streamflow data if they are available (it should be noted that both A_s and i_0 in equations (15) and (18) are not model parameters, they are evaluated at each time step). The other hydrological parameters can be estimated using, for instance, soil characteristics. Clearly, for application in GCMs, global parameter estimation using streamflow data is infeasible; for GCM applications *Dümenil and Todini* [1992] have suggested values for b_i, D_s, and W_s. An ongoing research topic, which will be investigated in the Global Energy and Water Experiment Continental Scale International Project (GCIP), is to develop regional relationships for GCM hydrological parameters. However, because streamflow data were available for Kings Creek, we made use of the observed data to estimate b_i, D_s, and W_s.

In order to estimate b_i, D_s, and W_s through calibration, we need to know $E_p[1]$ and $r_w[1]$, in addition to other parameters like W_j^c, W_j^w, W_j^{cr} (j=1, 2), K_s, B_p, θ_r, $f_1[1]$, $f_2[1]$, $u_n(z_2)$, $d_0[1]$, $z_0[1]$, $r_0[1]$, $r_{0c}[1]$, and LAI[1,m] (m=1, 2, . . . , 12). At the FIFE site, the data required to estimate $E_p[1]$ by the Penman-Monteith method and $r_w[1]$ by equation (3) are available only during the IFCs. Therefore for the purposes of estimating the hydrological parameters, we used Hamon's method [*Hamon et al.*, 1954; *Hamon*, 1961] which requires only daily air temperature and latitude to estimate $E_p[1]$. During summer 1987 we also used $E_p[1]$ via the Hamon method for the between-IFC periods to allow continuous computation of soil moisture (needed as initial values during the IFCs). The daily $E_p[1]$ computed using the Hamon formula was compared with the daily $E_p[1]$ obtained using Penman-Monteith's equation for the 35 days of the 1987 FIFE IFCs. The comparison indicated that the Hamon equation gives smaller $E_p[1]$ estimates, but the pattern over the 35-day period was similar for both $E_p[1]$ estimates. Therefore we scaled the Hamon estimates to have the same mean as the Penman-Monteith estimates, using an adjustment factor k_e, which was determined to have a mean of 1.64 with a standard deviation of 0.70 over the 35 days. The scaled Hamon estimates were used for the long-term hydrologic water balance computations, except during the IFC periods, when the data needed for computation of the Penman-Monteith $E_p[1]$ were available. During the IFC periods, $E_p[1]$ and $r_w[1]$ were estimated by the Penman-Monteith method and by equation (3), respectively.

For the 35 days of the IFCs, we calculated an average aerodynamic resistance (equal to the inverse of the product of the drag coefficient from equation (4b) and the wind speed under the assumption that the resistance to the transfer of momentum and water are equal). This average aerodynamic resistance was then used for the purpose of estimating the hydrological model parameters, and for computing the soil moisture at the beginning of the first IFC and between IFCs (but not for validation of the energy fluxes during the IFCs reported in section 4). The average aerodynamic resistance over the 35 days was 40.8 s/m with a standard deviation of 29.7 s/m. This value is within the range given for short grass and crops by *Monteith and Unsworth* [1990]. Since the roughness length of many crops decreases as wind speed increases, the inverse of aerodynamic resistance is approximately a constant over a range of low wind speeds. The daily average wind speed during the 35 days was 2.38 m/s, and the aerodynamic resistance (40.8 s/m) was taken as constant for the estimation of the three hydrological parameters. In addition, we did not correct for atmospheric stability, primarily to assure compatibility of $E_p[1]$ between the IFCs and during the longer period of hydrological water balance simulation, when the data needed to make the corrections were not available. However, the stability correction given by equations (3) and (4) was applied to the energy flux computations performed for the model validations reported in section 4.

At the FIFE site, the depths of layer 1 (upper zone) and layer 2 (lower zone) are about 0.5 m and 2.5 m, respectively (Famiglietti and Wood, submitted paper 1). Since the soil texture at FIFE is silt loam [*Environmental Protection Agency (EPA)*, 1991], the porosity was taken to be 0.5, and thus W_1^c =0.25 m and W_2^c =1.25 m, and W_j^w and W_j^{cr} are about 26% and 46% of the total water that the soil can hold. However, *Smith et al.* [1993] reported that evapotranspiration was not observed to be limited by soil moisture in the 20%-30% range, and they took 18% as the wilting point instead, which we also used as our estimate. In this study we used 70% of field capacity as our critical point (we found via sensitivity analysis that almost the same results were obtained when the critical point was 75% of field capacity). K_s, B_p, θ_r were taken as 6.44 mm/h, 0.16, and 0.01 m, respectively, following Famiglietti and Wood (submitted paper 1). Since the vegetation is dominated by grass, we assumed that all the roots are in the upper zone (i.e., $f_1[1]$=1.0 and $f_2[1]$=0.0).

Because the wind speed from the PAM stations was measured at 5.4 m above the ground surface, and the other meteorological data were measured at $z_2[1]$=2 m above ground surface, the wind speed was converted to the 2 m level through a logarithmic velocity profile. *Sugita and Brutsaert* [1990] estimated the zero plane displacement height $d_0[1]$=26.9 m, and the surface roughness length $z_0[1]$=1.05 m at FIFE by analyzing neutral wind velocity profiles measured by radiosondes. They found that a logarithmic velocity profile only holds over the

height ranges between 50 m ± 19 m and 202 m± 101 m above the ground surface. However, their values should be interpreted in the context of the Flint Hills region, which is characterized by relief of about 25 m between steep ridges and valleys. By contrast, *Smith et al.* [1992a] used much smaller local values of $d_0[1]$=0.25 m, and $z_0[1]$=0.07 m. Their values fall between uncut grass and long grass/crops for a relatively flat area [*Arya*, 1988]. Since the FIFE site is only a small part of the Flint Hills region which covers a 50- to 80-km-wide north-south strip in Kansas from Nebraska to Oklahoma, we decided to use the smaller values for $d_0[1]$ and $z_0[1]$, and assumed a logarithmic velocity profile locally. The 2-m wind speed can then be estimated as

$$u_n(z_2) = u_n(z_1)\frac{\ln\left(\frac{z_2[1]-d_0[1]}{z_0[1]}\right)}{\ln\left(\frac{z_1[1]-d_0[1]}{z_0[1]}\right)} \tag{39}$$

where $z_1[1]$=5.4 m, and $u_n(z_1)$ is the corresponding measured wind speed. The value of $r_0[1]$ for grassland is taken as 2.0 s/m [*Ducoudre et al.*, 1993]. *Monteith and Unsworth* [1990] suggest that for grassland $r_{0c}[1]$=100 s/m. *Smith et al.* [1993] found that both $r_{0c}[1]$=100 s/m and $r_{0c}[1]$=125 s/m are among the best values they obtained through an optimization, with the latter slightly better. Thus we take $r_{0c}[1]$=100 s/m. The monthly average LAI[1,m] (m=1, 2, . . . , 12) were derived from the average normalized difference vegetation index (NDVI) given by *EPA* [1991] with LAI_{max}=6.0 and LAI_{min}=0.1 which are consistent with the values used by *Smith et al.* [1993],

$$\mathrm{LAI}[1,m] = 0.1 + 0.0628(\mathrm{NDVI}[1,m] - 53.0) \tag{40}$$

The average monthly NDVIs for 1986, 1987, and 1988 at FIFE are listed in Table 1.

The hydrological parameter D_m can be either estimated by identifying extended dry periods during the calibration interval 1982-1985 using the precipitation data, and recession rates inferred from the observed Kings Creek streamflows during these periods; or by multiplying saturated hydraulic conductivity by an average soil slope. We used the first approach, which gave D_m = 8.2 mm/d. The hydrological parameters b_i and D_s, and W_s, were estimated using streamflow at Kings Creek, and precipitation, and maximum/minimum temperature data at Manhattan, Kansas from 1982-1985. The calibration gave b_i=0.008, D_s=7.7×10 $^{-5}$, and W_s=0.96. It should be mentioned that the one-layer snowmelt model was not used to obtain the above model parameters, since not much snow occurs in the Kings Creek catchment. Hydrographs for two of the calibration years (1983 and 1984) are shown in Figures 4a and 4b. The model reproduces the streamflow reasonably well; discrepancies are attributed to (1) the distance of the precipitation gage from the Kings Creek catchment; (2) the inability of a single gage to represent spatial variations in precipitation; (3) the use of a daily time step for a relatively small catchment whose time of concentration is of the order of an hour or less; and (4) small-scale heterogeneities which can strongly affect runoff production in small catchments and are not captured by a macroscale model such as VIC.

With the parameters described above, together with the parameters $\alpha[1]$, $\kappa[1]$, $C_s[1]$, D_2, and T_2, we then used the PAM and flux data to test our model-predicted surface fluxes and surface temperature against with the measured ones. The albedo $\alpha[1]$ was taken as 0.2 during the IFCs following Famiglietti and Wood (submitted paper 1). The thermal conductivity $\kappa[1]$ and soil heat capacity $C_s[1]$ in equation (33) were estimated to be 0.514 W m^{-1} K^{-1} and 2.13×10^6 J m^{-3} K^{-1}, respectively, following *Smith et al.* [1992b, 1993]. The depth D_2 was taken to be 0.45 m, and the temperature T_2 (i.e., T_{50}) in equation (33) was prescribed as 293.6 °K, which was the average of T_{50} for the selected 35 days of the IFCs. The standard deviation of T_{50} for the 35 days was 3.1 °K . All the values of the hydrologically and atmospherically related model parameters are listed in Table 2. We compared the surface energy budgets computed using both equation (25) and equation (27), and found that there was almost no difference in the results when we took $z_a[1]$=$z_2[1]$=2 m.

4. Model Validation

Figures 5a and 5b show predicted and observed streamflow for 1986 and 1987, 2 years not in the calibration period. Generally, the results are consistent with those of the calibration period: the dry period flows are fairly well represented, as is the timing of the major peaks, but the magnitudes of the peaks, especially the largest ones, are subject to major errors. In this study, streamflow prediction is not a goal per se, instead, our purpose in evaluation of the predicted hydrographs is to provide evidence that the model is producing a reasonable soil water balance. To this extent, the hydrograph simulations were judged adequate.

After estimating the hydrological model parameters, we used the FIFE surface fluxes and meteorological measurements for the summer of 1987 to test the model predictions of latent heat, sensible heat and ground heat fluxes, and the surface temperature. We used the Kings Creek precipitation network, as well as the precipitation, air temperature, and downward solar and long-wave radiation composited from the PAM and flux stations by *Betts et al.* [1993] to test the model heat fluxes and surface temperature. Results are shown in Figures 6, 7, and 8 for parts of the June, July, August, and October IFCs.

Figure 6 shows part of IFC 2 (from June 30 - July 11). There were precipitation events on June 30 and July 7. On the rest of the days, there was little or no rainfall. During this period, the latent heat flux for dry days was typically about 400 W m^{-2} . The model predicted the latent heat and sensible heat fluxes fairly well, except that it somewhat underpredicted the July 9, 10, and 11 latent heat fluxes and overpredicted the sensible heat fluxes on the same days. These days were characterized by relatively high winds, high potential evaporation, and high soil moisture. The surface temperatures agree with the observed ones quite well, but the magnitude of the diurnal cycle of the ground heat flux was underpredicted on some of the days.

Figure 7 shows predicted and observed latent, sensible, and ground heat fluxes, and surface temperature, for the August 9-20, 1987, portion of the third IFC. Rainfall occurred on August 12, 13 and 18. Before the August 12-13 storm, the soil was moderately dry. During this period, the observed latent heat fluxes were less than 300 W m^{-2}. After the rainfall, the latent heat fluxes increased to about 400 W m^{-2}. During this period, the model predicted the latent heat and sensible heat fluxes quite well, except during the nights of August 14 and 15, when the latent heat fluxes were overpredicted and the sensible heat fluxes were underpredicted. This is mainly due to the high

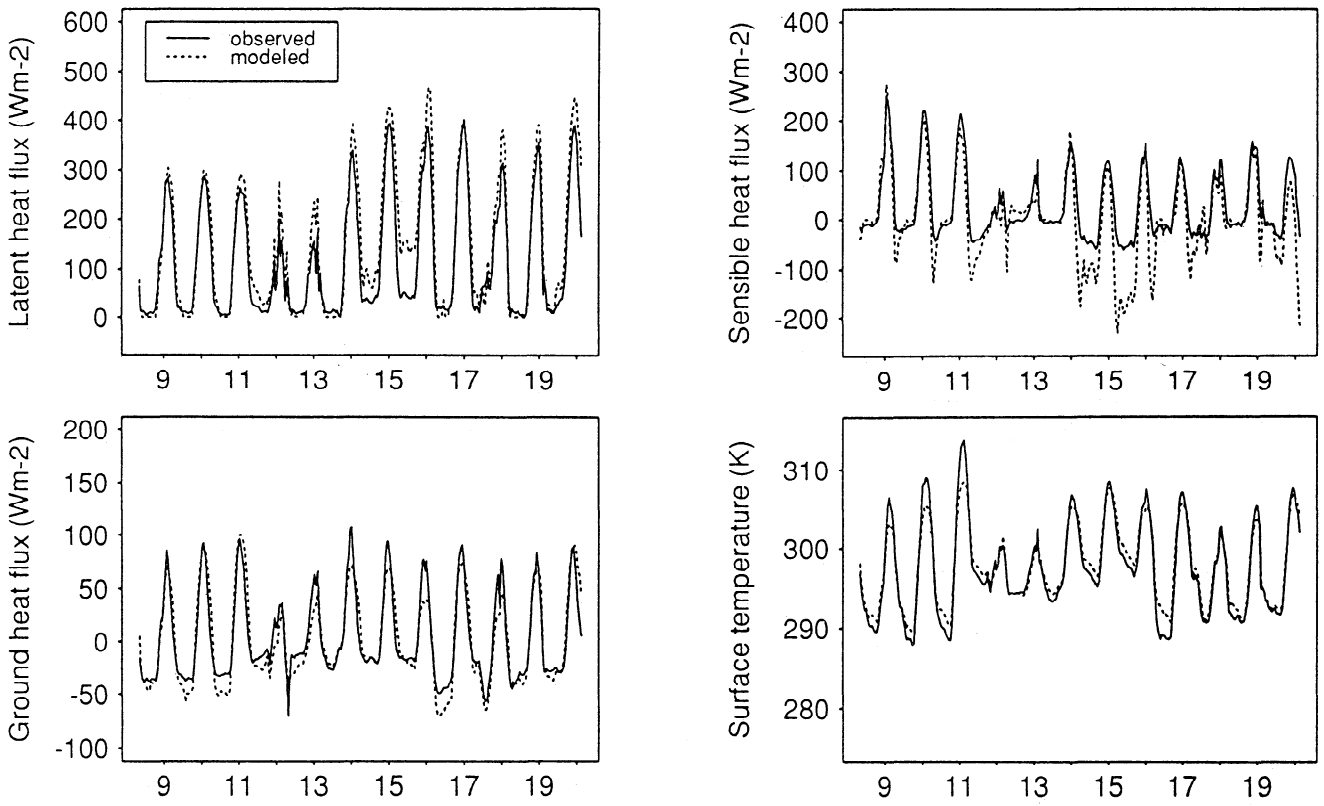

Figure 7. Comparison of predicted (dotted) and observed (solid) surface fluxes and surface temperature at the FIFE site for August 9-20, 1987 (IFC 3).

potential evaporation obtained during that time. From equations (1) and (5), it can be seen that large evaporation would be obtained if the potential evaporation is large, even though the $r_w[n]$ and $r_c[n]$ are reasonable. During this period, the ground heat fluxes were predicted reasonably well, although there was a tendency to underestimate the magnitude of the diurnal cycle. The surface temperatures were well predicted in general.

Figure 8 shows the energy fluxes and surface temperature for October 6-16, 1987, a portion of IFC 4 which was characterized by low soil moisture. During this period, the observed latent heat fluxes were about 100 W m^{-2} or less, while the sensible heat fluxes increased to about 300 W m^{-2} (from about 200 W m^{-2} in July and August). The model predicts the latent and sensible heat fluxes, and surface temperature, reasonably well, but it overpredicts the ground heat fluxes on most of the days during this period.

In general, the model performed quite satisfactorily, especially given its simplicity. There are some caveats in interpretation of the results. First, the FIFE site is a native grassland, which is characterized by a single vegetation type. Therefore the portion of the model dealing with heterogeneous vegetation was not exercised in these tests, so the effects of certain associated simplifications are not reflected in the results. A second, related limitation is that since the FIFE vegetation is all grassland, the algorithms dealing with trees, which usually extract moisture from the lower, rather than the upper, soil moisture zone have not been exercised. We have, however, implemented the model for a tropical forest application in connection with the Project for Intercomparison of Land-surface Parameterization Schemes [*Pitman et al.*, 1993; *Liang et al.*, 1993], and the model results were comparable to those of most of the participating models.

5. Conclusions

We have described a land surface model designed for application within coupled land-atmosphere-ocean GCMs. The model is formulated to be applied as a fully coupled water and energy balance system. The land surface hydrology is a generalization of the VIC (variable infiltration capacity) model which incorporates a two-layer description of the soil column, in which the upper layer is characterized by the usual VIC spatial distribution of soil moisture capacities, and the lower layer is spatially lumped, and uses the Arno [*Francini and Pacciani*, 1991] drainage term. The model partitions the area of interest (e.g., grid cell) into N+1 land surface cover types; for each land cover type the fraction of roots in the upper and lower zone is specified. Evaporation and transpiration are parameterized by a Penman-Monteith formulation, applied separately to bare soil and vegetation classes. Evaporation from water intercepted by the vegetation is also represented. In addition, the model contains an energy-based snow accumulation and ablation parameterization.

Although the model is formulated for a fully coupled application within a GCM, it can also be run "off-line" using observed energy and water fluxes (or their surrogates, especially in the case of radiation forcings) as forcings. The importance of off-line simulation for this particular model is that it allows that hydrologic parameters to be calibrated so as to maintain long-term, observed water balances. This was accomplished, in the absence of long-term (multiple year) radiation data, using surface air temperature as a surrogate (via Hamon's method) to estimate the potential evapotranspiration. With estimates of potential evapotranspiration, the land surface hydrology parameters can be estimated using observed precipitation and streamflow. This approach is an important

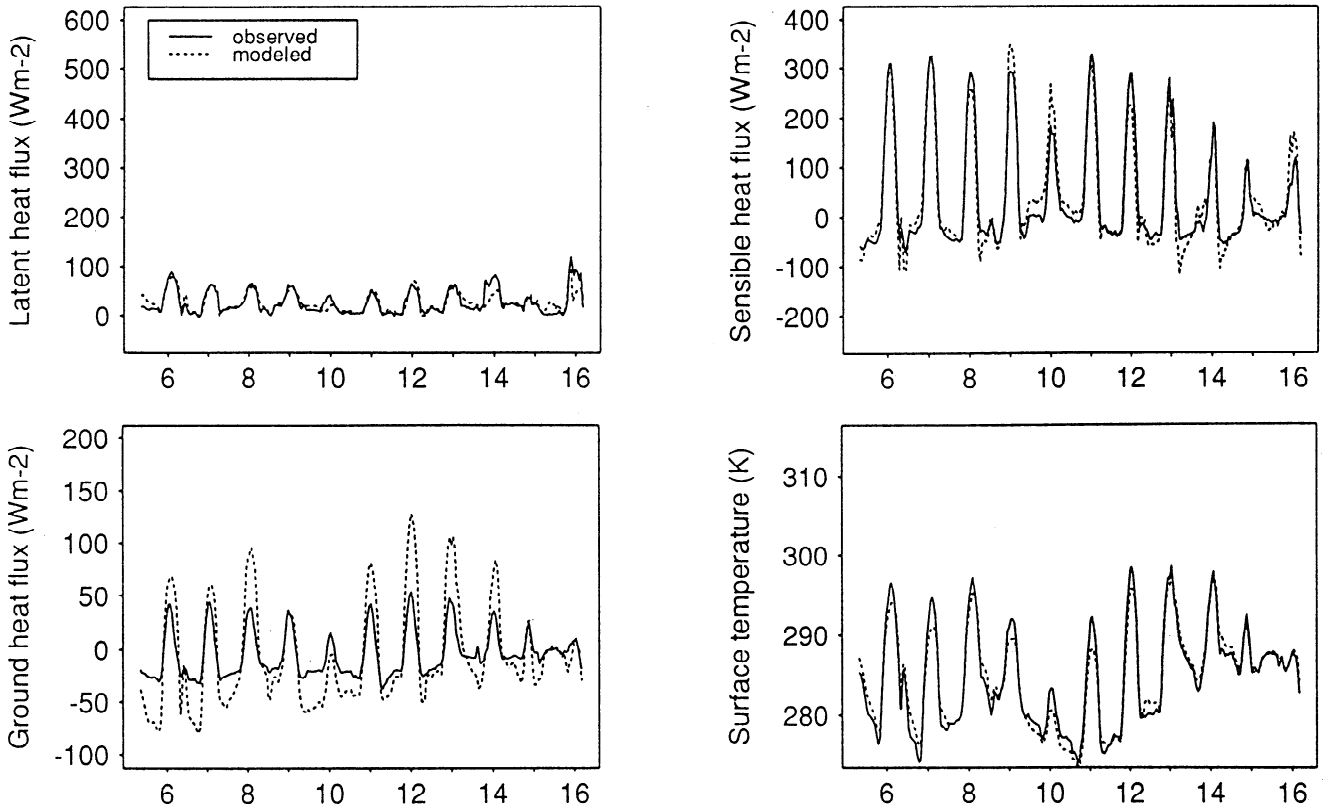

Figure 8. Comparison of predicted (dotted) and observed (solid) surface fluxes and surface temperature at FIFE site for period of extremely dry soil moisture during October 6-16, 1987 (IFC 4).

step to application of improved land surface schemes within GCMs, since it offers the possibility of mapping the hydrologic parameters globally using well-established regionalization methods.

We tested the approach using long-term hydrologic and climatalogical data for Kings Creek, Kansas; the estimated surface energy fluxes were then tested using FIFE data for selected days of the 1987 IFCs. The model performed quite well, giving encouragement that the VIC approach to parameterizing the spatial variability in the land surface properties, coupled with a simplified vegetation model, may be sufficient to represent the land surface fluxes at the GCM scale. Nonetheless, it must be emphasized that the model testing to date is for a small area and a specific land cover and climate; further testing will be required at other sites where detailed surface flux data are available before the model can be considered to be globally validated. This latter concern, however, is not limited to our model alone; a major thrust of such projects as GCIP, and large-scale field experiments such as Boreal Ecosystem-Atmosphere Study (BOREAS), is to provide better large area surface moisture and energy flux data for validation of GCM land surface algorithms. The approach we have reported may be considered as a candidate protocol for future validations of GCM land surface parameterizations.

Acknowledgments. The research reported herein was supported in part by the U.S. Environmental Protection Agency under Cooperative Agreement 816335-01-0, by Pacific Northwest Laboratory under contract DE-AC06-76RLO 1830 with the U.S. Department of Energy, and NASA under contracts NAGW-2556 and NAS5-31719.

References

Arya, S.P., *Introduction to Micrometeorology*, 307 pp., Academic, San Diego, Calif., 1988.

Avissar, R., and R.A. Pielke, A parameterization of heterogeneous land surface for atmospheric numerical models and its impact on regional meteorology, *Mon. Weather Rev., 117*, 2113-2136, 1989.

Betts, A.K., J.H. Ball, and A.C.M. Beljaars, Comparison between the land surface response of the ECMWF model and the FIFE-1987 data, *Q. J. R. Meteorol. Soc., 119*, 975-1001, 1993.

Blondin, C., Parameterization of land-surface processes in numerical weather prediction, in *Land Surface Evaporation: Measurements and Parameterization*, edited by T.J. Schmugge and J.C. Andre, pp. 31-54, Springer-Verlag, New York, 1991.

Brooks, R.H., and A.T. Corey, Hydraulic properties of porous media, *Hydrol. Pap. 3*, Colo. State Univ., Ft. Collins, 1964.

Deardorff, J.W., Efficient prediction of ground surface temperature and moisture, with inclusion of a layer of vegetation, *J. Geophy. Res., 83*, 1889-1903, 1978.

Dickinson, R.E., Modelling evapotranspiration for three-dimensional global climate models, in *Climate Processes and Climate Sensitivity, Geophys. Monogr. Ser.*, vol. 29, edited by J.E. Hansen and T. Takahashi, pp. 58-72, AGU, Washington, D.C., 1984.

Dickinson, R.E., A. Henderson-Sellers, P.J. Kennedy, and M.F. Wilson, Biosphere-atmosphere transfer scheme (BATS) for the NCAR community climate model, *NCAR Tech. Note, TN-275+STR*, 1986.

Ducoudre, N.I., K. Laval, and A. Perrier, SECHIBA, a new set of parameterizations of the hydrologic exchanges at the land-atmosphere interface within the LMD atmospheric general circulation model, *J. Clim., 6*, 248-273, 1993.

Dümenil, L., and E. Todini, A rainfall-runoff scheme for use in the Hamburg climate model, in *Advances in Theoretical Hydrology,*

A Tribute to James Dooge, edited by J.P. O'Kane, pp. 129-157, European Geophysical Society Series on Hydrological Sciences, 1, Elsevier, New York, 1992.

Entekhabi, D., and P.S. Eagleson, Land surface hydrology parameterization for atmospheric general circulation models including subgrid scale spatial variability, *J. Clim., 2*, 816-831, 1989.

Environmental Protection Agency (EPA), Global ecosystems database documentation, in *EPA Global Climate Research Program NOAA/NGDC Global Change Database Program*, EPA Res. Lab., Corvallis, Ore., 1991.

Francini, M., and M. Pacciani, Comparative analysis of several conceptual rainfall-runoff models, *J. Hydrol., 122*, 161-219, 1991.

Hamon, R.W., Estimating potential evapotranspiration, *J. Hydraulics Div., Am. Soc. Civ. Eng., 87*, 107-120, 1961.

Hamon, R.W., L.L. Weiss, and W.T. Wilson, Insolation as an empirical function of daily sunshine duration, *Mon. Weather Rev., 82*, 141-146, 1954.

Liang, X., D.P. Lettenmaier, and E.F. Wood, A two-layer variable infiltration capacity land surface parameterization for GCMs, paper presented at '93 Joint International Meeting, IAMAP·IAHS, Yokohama, Japan, July 1993.

Louis, J., A parametric model of vertical eddy fluxes in the atmosphere, *Boundary Layer Meteorol., 17*, 187-202, 1979.

Manabe, S., Climate and the ocean circulation, I, The atmospheric circulation and the hydrology of the Earth surface, *Mon. Weather Rev., 97*, 739-774, 1969.

Monteith, J.L., and M.H. Unsworth, *Principles of Environmental Physics*, 291 pp., 2nd ed., Routledge, Chapman and Hall, New York, 1990.

Pitman, A.J., et al., Project for intercomparison of land-surface parameterization schemes (PILPS): Results from off-line control simulation (phase 1a), *GEWEX WCRP, IGPO Pub. Series No. 7*, 1993.

Saugier, B., and N. Katerji, Some plant factors controlling evapotranspiration, *Agric. and Forest Meteorol.*, 54, 263-277, 1991.

Sellers, P.J., Y. Mintz, Y.C. Sud, and A. Dalcher, A simple biosphere model (SiB) for use within general circulation models, *J. Atmos. Sci., 43*(6), 505-531, 1986.

Sellers, P.J., F.G. Hall, G. Asrar, D.E. Strebel, and R.E. Murphy, An overview of the First International Satellite Land Surface Climatology Project (ISLSCP) Field Experiment, *J. Geophys. Res., 97*(D17), 18,345-18,371, 1992.

Shuttleworth, W.J., Evaporation, in *Handbook of Hydrology*, edited by D.R. Maidment, pp. 4.1-4.53, McGraw-Hill, Inc., New York, 1993.

Smith, E.A., W.L. Crosson, and B.D. Tanner, Estimation of surface heat and moisture fluxes over a prairie grassland, 1, In situ energy budget measurements incorporating a cooled mirror dew point hygrometer, *J. Geophys. Res., 97*(D17), 18,557-18,582, 1992a.

Smith, E.A., et al., Area-averaged surface fluxes and their time-space variability over the FIFE experimental domain, *J. Geophys. Res., 97*(D17), 18,599-18,622, 1992b.

Smith, E.A., H.J. Cooper, W.L. Crosson, and H. Weng, Estimation of surface heat and moisture fluxes over a prairie grassland, 3, Design of a hybrid physical/remote sensing biosphere model, *J. Geophys. Res., 98*(D3), 4951-4978, 1993.

Stamm, J.F., E.F. Wood, and D.P. Lettenmaier, Sensitivity of a GCM simulation of global climate to the representation of land surface hydrology, *J. Clim.*, in press, 1994.

Sugita, M., and W. Brutsaert, Wind velocity measurements in the neutral boundary layer above hilly prairie, *J. Geophys. Res., 95*, 7617-7624, 1990.

Wigmosta, M., L. Vail, and D.P. Lettenmaier, A distributed hydrology-vegetation model for complex terrain, *Water Resour. Res.*, in press, 1994.

Wood, E.F., Global scale hydrology: Advances in land surface modeling, *U.S. Natl. Rep. Int. Union Geod. Geophys. 1987-1990, Rev. Geophys., 29*, Supplement, 193-201, 1991.

Wood, E.F, D.P. Lettenmaier, and V.G. Zartarian, A land-surface hydrology parameterization with subgrid variability for general circulation models, *J. Geophys. Res., 97*(D3), 2717-2728, 1992.

Xue, Y., P.J. Sellers, J.L. Kinter, and J. Shukla, A simplified biosphere model for global climate studies, *J. Clim., 4*, 345-364, 1991.

Zhao, R.-J., Y.-L. Zhang, L.-R. Fang, X.-R. Liu, and Q.-S. Zhang, The Xinanjiang model, Hydrological Forecasting Proceedings Oxford Symposium, IASH 129, pp. 351-356, 1980.

S. J. Burges, D. P. Lettenmaier, and X. Liang, Department of Civil Engineering, FX-10, University of Washington, Seattle, WA 98195 (e-mail: sburges@u.washington.edu; 52018@u.washington.edu; xliang@u.washington.edu)

E. F. Wood, Department of Civil Engineering and Operations Research, Princeton University, Princeton, NJ 08544 (efwood@pucc)

(Received February 6, 1993; revised January 11, 1994; accepted February 14, 1994.)